Catalysis Today 151 (2010) 376–385

Contents lists available at ScienceDirect

Catalysis Today

journal homepage: www.elsevier.com/locate/cattod

NO_x removal over a double-bed NSR-SCR reactor configuration

R. Bonzi, L. Lietti *, L. Castoldi, P. Forzatti

Dipartimento di Energia, Laboratory of Catalysis and Catalytic Processes and NEMAS, Centre of Excellence, Politecnico di Milano, P.zza L. da Vinci 32, Milano, Italy

ARTICLE INFO

Article history:
Available online 7 March 2010

Keywords:
Lean deNO_x
NO_x reduction mechanism
LNT systems
Pt–Ba/Al_2O_3 catalyst
Combined LNT + SCR catalysts

ABSTRACT

A detailed analysis of the catalytic behaviour in the storage/reduction of NO_x of single Pt–Ba/Al_2O_3 LNT and FeZSM-5 SCR systems and of combined LNT + SCR configurations is analyzed and compared in this work under clean conditions (i.e. in the absence of CO_2 and H_2O in the feed stream). By working under dilute conditions (i.e. with low reductant concentrations) and with an inert purge between the lean and the rich phases, nearly ideal isothermal conditions could be attained and the chemical pathways operating in the each step of the NSR cycle could be analyzed for the investigated catalysts configurations. It is found that when the SCR catalyst is placed downstream the NSR catalyst bed (double-bed configuration), ammonia released from the LNT sample during the rich phase is stored on the SCR catalyst placed downstream and is then converted to N_2 in the subsequent lean phase according to the occurrence of a SCR reaction. This has a benefit on both the NO_x removal efficiency and the N_2 selectivity. If the zeolite SCR catalyst is mixed with the LNT sample (physical mixture), during the rich phase the SCR catalyst traps ammonia which being intermediate in N_2 formation leads to a decrease in the evolution of nitrogen at the reactor outlet. Ammonia stored on the SCR catalyst then reacts with NO_x during the subsequent lean phase, leading to a significant N_2 evolution: this increases the NO_x removal efficiency and the N_2 selectivity if compared to the single Pt–Ba/Al_2O_3 catalyst sample.

1. Introduction

Diesel-equipped vehicles are one of the primary sources of NO_x and particulate (soot) emissions in industrialized countries. Accordingly regulations to limit their emissions are becoming very strict: in Europe, the Euro V rules impose limits in the particulate and NO_x emissions of 0.005 and 0.18 g/km, respectively. A further decrease in the NO_x emission, down to 0.08 g/km, will be imposed by the next-coming Euro VI rules in 2014.

Soot emissions control is generally achieved by the use of the so-called DPF (Diesel Particulate Filter) devices [1]. On the other hand, different solutions have been proposed for the abatement of NO_x under lean conditions [1]. A possibility is the urea-SCR system, which can eliminate NO_x emission from diesel exhaust gases with high efficiency. However, due to its technical complexity, this technology is preferably applicable to trucks and heavy-duty vehicles [2], although applications for passenger cars have also been proposed [1].

In the urea/SCR technology, urea is injected in the flue gases where it decomposes and hydrolyzes to CO_2 and NH_3. The typical SCR process is based on the following reaction between NH_3 and NO, the so-called "standard SCR" reaction:

$$2NO + 2NH_3 + 1/2O_2 \rightarrow 2N_2 + 3H_2O \qquad (1)$$

However, if NO_2 is present in the exhaust gases, e.g. when an oxidation catalyst is located upstream of the SCR catalyst, the so-called "fast-SCR" reaction (2) can also occur, which is considerably faster than reaction (1):

$$NO + NO_2 + 2NH_3 \rightarrow 2N_2 + 3H_2O \qquad (2)$$

Metal-substituted zeolites, such as FeZSM-5, are among the most active catalysts for the urea/NH_3-SCR process [3,4].

In order to overcome the problems associated to the use of urea (i.e. the need to have a reservoir of NH_3, or its precursor, and the complexity of the ammonia feeding system) the so-called NO_x storage–reduction (NSR) systems, also known as Lean NO_x Traps (LNTs), have also been proposed. To achieve the reduction of NO_x in fuel-lean (i.e. oxygen-rich) atmosphere, NSR utilizes unsteady state operation by switching between long fuel-lean and short fuel-rich conditions [5,6]. Conventional NSR catalysts consist of precious metal and alkaline/alkaline-earth metal, typically platinum and barium, respectively, finely dispersed on metal oxide supports, e.g. γ-alumina. During lean periods nitric oxide present in the flue gases reacts with oxygen to produce nitrogen dioxide on Pt particles, and the so-formed NO_2 is captured by Ba components as nitrites and nitrates. In parallel with the above mechanism,

---

* Corresponding author. Tel.: +39 02 2399 3272; fax: +39 02 7063 8173.
E-mail address: luca.lietti@polimi.it (L. Lietti).

0920-5861/$ – see front matter © 2010 Elsevier B.V. All rights reserved.
doi:10.1016/j.cattod.2010.02.003

direct NO storage on BaO assisted by O_2 and Pt has been also proposed [7]. The stored NO_x are then reduced to N_2 during a short fuel-rich period (usually few seconds) [6]. During the dynamic processes of NSR, the participation of several types of Ba species, i.e. BaO, $Ba(NO_3)_2$, $Ba(NO_2)_2$, $BaCO_3$, and $Ba(OH)_2$, has been suggested [8,9].

The chemistry and mechanisms involved in the reduction of the stored NO_x are still a matter of debate. Recently, it has been suggested that ammonia is intermediate in the reduction of the stored nitrates by H_2 under isothermal conditions [10–12]. A reaction pathway has been proposed which is able to account for both the high initial N_2 selectivity of the reaction and the temporal sequence of the products observed during the rich operation, with NH_3 evolution following that of N_2. In particular, it has been shown that an H_2 front develops in the trap during the rich phase [10,13,14], which travels along the reactor axis. Clear evidences have been provided on the fact that N_2 formation involves the occurrence of an in-series two step molecular process involving at first the formation of NH_3 upon reaction of H_2 with the stored nitrates, followed by the reaction of the so-formed ammonia with nitrates located downstream the H_2 front. This reaction leads selectively to N_2. Accordingly the regeneration of the trap proceeds both in the part of the reactor in which nitrates are reduced by H_2 to give ammonia and in the zone in which the ammonia formed upstream reacts with nitrates leading to N_2. Notably, step 1 (i.e. NH_3 formation) has been found to be much faster than the second step, that is nitrogen formation via reaction of nitrates with NH_3. Accordingly if regeneration of the trap is carried out at low temperatures (i.e. near 200 °C) the reaction of NH_3 with the stored nitrates does not take place and ammonia leaves the catalyst unreacted, leading to significant NH_3 emissions (NH_3 slip).

This pathway explains why the NH_3 release from LNTs depends on the reaction temperature. To avoid the ammonia slip, an ammonia oxidation catalyst may be placed downstream the LNT catalyst, to oxidize the released NH_3 to N_2. A different option is to place a NH_3-SCR catalyst layer downstream the NSR catalyst. In this case the NH_3 released from the NSR catalyst during the rich phase is adsorbed on the SCR bed; the stored ammonia then reacts with gaseous NO according to the NH_3-SCR reaction (1) during the subsequent lean cycle. As recently demonstrated, the use of this double-bed configuration effectively increases both the N_2 selectivity and the NO_x removal efficiency if compared to a single NSR catalyst layer [15–17].

In spite of the fact that the advantages of the use of combined NSR + SCR systems have already been recognized, still many aspects of the reaction pathways operating during both the lean and the rich phases in these coupled catalyst configurations need to be further clarified. In recent papers published by Corbos et al. [18,19], the authors documented the improvement of the catalytic performances in the NO_x removal when an in-series NSR and SCR catalyst configuration has been used, if compared to a single catalyst layer. The authors also showed that some benefits in the NO_x abatement efficiency could be obtained by physically mixing the NSR and SCR catalysts, particularly when using CO as a reductant. The experiments carried out by Corbos et al. have been performed close to real operating conditions, i.e. by alternating long lean phases with short rich periods with high reductant concentration, and this gives rise to relevant temperature effects during the lean/rich cycles. Besides, the FTIR analyzer used by the authors could not monitor N_2 formation, and this did not allow the complete analysis of the products.

Accordingly, a systematic study has been carried out in our laboratories in which the reactivity in the NO_x storage and reduction phases has been investigated over single NSR (Pt–Ba/Al_2O_3) and SCR (FeZSM-5) catalyst layers, and over combined catalyst configurations as well (i.e. a double-bed configuration with the NSR catalyst layer placed upstream the SCR catalyst and a physical mixture of the two catalyst samples in one layer). Goal of our investigation was to provide a deeper analysis on the pathways operating during both the lean (NO_x storage) and the rich (catalyst regeneration) operation on the considered NSR/SCR catalyst combination. In particular, we wanted to rationalize the behaviour of the combined LNT/SCR catalytic systems on the basis of the proposed pathways for the reduction of the stored NO_x which suggest the participation of NH_3 as intermediate species. In order to decouple the various effects, and to avoid any artefacts originating from uncontrolled temperature increases upon lean/rich cycling, experiments have been performed under nearly isothermal conditions, i.e. in the absence of significant temperature effects upon lean/rich cycling. This has been accomplished by using low reductant concentrations and by separating the lean and the rich phases by an inert purge in between. Besides, the whole spectrum of reaction products has been analyzed, including N_2. Accordingly a more precise rationalization of the catalytic behaviour and a better understanding of the chemical processes occurring during the lean/rich cycling could be obtained. Experiments have been carried out under “clean” conditions, i.e. in the absence of water and CO_2 in the feed stream; the role of these components is presently under investigation and results will be reported in a forthcoming paper.

2. Experimental

2.1. Catalysts preparation and characterization

A homemade Pt–Ba/Al_2O_3 (1/20/100, w/w) catalyst has been used in this study. The catalytic system has been prepared by incipient wetness impregnation of a commercial alumina sample (Versal 250 from UOP) with aqueous solution of dinitro-diammine platinum (Strem Chemicals, 5% Pt in ammonium hydroxide) and subsequently with a solution of barium acetate (Aldrich, 99%). The powder has been dried at 80 °C and calcined in air at 500 °C for 5 h after each impregnation step [8,20]. The impregnation order (first Pt and then Ba) has been selected in order to ensure a good dispersion and stability of the noble metal and of the alkaline component on the alumina support, in line with recipes of Toyota patents [21].

The SCR catalyst is a FeZSM-5 sample purchased from Zeolyst International (Fe loading near 1%, w/w). The FeZSM-5 sample has been calcined in air at 500 °C for 5 h.

Both powder catalysts have been characterized by XRD, surface area and pore size measurements. XRD diffraction spectra have been recorded with a Philips PW 1050/70 diffractometer equipped with a vertical goniometer using a Ni-filtered Cu Kα radiation. Surface area and pore size distribution have been determined by N_2 adsorption–desorption at 77 K with the BET method using a Micromeritics TriStar 3000 instrument. For the Pt–Ba/Al_2O_3 catalyst, the Pt dispersion has also been measured by hydrogen chemisorption at 0 °C, after reduction in H_2 at 300 °C, using a TPD/R/O 1100 Thermo Fischer Instrument.

2.2. Catalytic tests

All catalytic tests have been performed with powder catalysts (sieved at 70–100 μm) loaded in a quartz micro-reactor tube (8 mm ID), directly connected to a mass spectrometer (QMS 200, Pfeiffer) for complete analysis of reactants and products, including N_2 and NH_3 [7,8,22]. The detection of NH_3 is affected by a small delay, due to its adsorption on the Mass Spec capillary probe as pointed out by blank experiments; however this delay can be neglected in the results discussed below.

The tests have been performed using single catalyst beds (NSR or SCR), a double-bed LNT + SCR arrangement (in which the FeZSM-5 SCR catalyst is placed downstream the Pt–Ba/Al_2O_3 sample, separated by a quartz plug) and a physical mixture of the two catalysts. In the case of the single-bed experiments 60 mg of catalyst have been loaded into the reactor, whereas in the case of the double-bed and the mechanical mixture configuration 60 mg of each catalyst sample have been used (total catalyst loading of 120 mg). In all catalytic arrangements, a flow of 100 cm^3/min (at 1 atm and 0 °C) has been used.

The catalyst temperature has been measured by means of a thermocouple (Type K) directly immersed in the catalyst bed; in the case of the double-bed experiments the thermocouple has been located in the upper catalyst bed.

ISC (Isothermal Step Concentration) experiments have been performed for all configurations of the catalytic beds. In these experiments, a sequence of lean and rich phases has been fed to the reactor, separated by an inert purge. During the lean phase, a pulse of NO (1000 ppm) has been admitted to the reactor in flowing He + O_2 (3%, v/v) until catalyst saturation. Then the NO concentration has been reduced to zero and when the NO signal reached the background level the oxygen flow was also stopped. Then after a He purge at the same temperature, the catalyst regeneration (rich phase) has been carried out with H_2 (2000 ppm in He). Before each test, the catalyst samples have been conditioned by performing a few adsorption/regeneration cycles. Conditioning lasted until a reproducible behaviour has been obtained; this typically required 2–3 cycles.

Note that due to the low reductant concentration employed in our experiments, thermal effects have been found to be negligible upon lean-rich cycling (<2 °C). Accordingly the experiments have been performed under nearly isothermal conditions.

Lean-rich cycles have been carried out at different temperatures, in the range 150–350 °C. For the sake of brevity, only the results obtained at the temperature of 200 °C are herein illustrated, since at this temperature the largest differences in the various catalyst configurations have been observed. However qualitatively similar results have been obtained also at different temperatures; this will be the object of a forthcoming paper.

In each lean-rich cycle, the NO_x removal efficiency and the N_2 selectivity have been calculated. The NO_x removal efficiency is the total amount of N-containing products detected at the reactor outlet (N_2, NH_3 and N_2O) rationed to the total amount of NO_x fed to the reactor during a lean-rich cycle. Note that in the case of the single-bed LNT catalyst, since negligible amounts of NO_x are released during the rich phase, the amounts of NO_x converted correspond to those stored onto the catalyst surface during the lean phase, which in fact are then reduced during the subsequent rich phase. On the other hand, in the case of the combined LNT/SCR systems (both double-bed and physical mixture), NO_x are stored during the lean phase (in the form of nitrites-nitrates) on the LNT catalyst, but also react with NH_3 stored on the SCR catalyst (see below). In this case the net amount of NO_x stored (on the NSR catalyst) is calculated as follows:

$$NO_x{}^{Stored} = NO_x{}^{Removed} - N_2{}^{Lean\,phase} \tag{a}$$

where $NO_x{}^{Stored}$ are the amounts of NO_x stored on the catalyst surface during the lean phase, $NO_x{}^{Removed}$ are the overall amounts of NO_x consumed (by adsorption and reaction) during the lean phase and $N_2{}^{Lean\ phase}$ are the amounts of N_2 formed during the lean phase according to the SCR reactions (1) and (2), which imply a 1/1 ratio between NO_x consumed and N_2 formed.

The selectivity to N_2 of the reduction process has also been estimated. Since the N_2 selectivity changes during the rich phase due to the variation in the products distribution with time, a time-weighted N_2 average selectivity has been calculated according to Eq. (b):

$$S_{N_2} = \frac{2n_{N_2}}{2n_{N_2} + n_{NO} + n_{NH_3}} \tag{b}$$

where n_{N_2}, n_{NO} and n_{NH_3} are the total molar amounts of N_2, NO and NH_3, respectively, evolved during the rich phase, and calculated by the integrals of the corresponding concentration vs. time curves. N_2O concentration has always been found negligible and accordingly this species has not been included in Eq. (b).

The N-balance, estimated by comparing the amounts of NO_x removed during the lean phase with those of the N-containing species formed during both the lean and rich phase, always closed within 10%, being typically lower than 5%.

Finally, the FeZSM-5 SCR catalyst has also been tested in the reactivity of the SCR reaction. For this purpose, a sequence of NH_3 (1000 ppm in He) and NO (1000 ppm in He + 3% O_2) pulses have been fed to the reactor at different temperatures, in the range 150–350 °C, with an inert purge in between.

3. Results and discussion

3.1. Catalyst characterization

The specific surface area of the commercial alumina sample after calcination at 700 °C is near 200 m^2/g, while a slightly lower value has been determined for the Pt–Ba/Al_2O_3 sample (160 m^2/g). The surface area contraction was not accompanied by significant changes in the pore volume (0.96 cm^3/g for γ-Al_2O_3 and 0.78 cm^3/g for Pt–Ba/Al_2O_3). The pore radius is in the range 90–110 Å.

In the XRD patterns of the calcined Pt–Ba/Al_2O_3 catalyst characteristic peaks of γ-Al_2O_3 (JCPDS 10-425) have been detected along with crystalline phases related to Ba-carbonate species [7,23]. The Pt dispersion measured by H_2 chemisorption was near 15%.

The FeZSM-5 SCR catalyst sample shows a specific surface area of 300 m^2/g, and pore volume of 0.11 cm^3/g. The XRD analysis reveals the characteristic peaks of the ZSM5 zeolite [24]; no reflections of Fe phases have been found. The iron content, estimated by atomic absorption spectrometry (Varian Spectra AA 110) after dissolving the sample in an acid solution, is near 1%.

3.2. Catalytic activity

3.2.1. NO_x storage–reduction over Pt–Ba/Al_2O_3

Lean-rich cycles have been performed over the Pt–Ba/Al_2O_3 conditioned catalyst at different temperatures; in Fig. 1 the results obtained at 200 °C are reported.

Upon NO admission to the reactor (t = 0 s in the right side of Fig. 1) the NO breakthrough is observed after 33 s. The NO concentration slowly increases with time and eventually reaches the inlet NO concentration value after about 1500 s. A small NO_2 formation, due to NO oxidation over the Pt component, is observed at this temperature:

$$NO + 1/2O_2 \rightarrow NO_2 \tag{3}$$

During NO adsorption the evolution of water is also observed. As discussed elsewhere [8], this is due to the uptake of NO_x on $Ba(OH)_2$ sites, accompanied by the release of H_2O.

When the NO signal shows a steady value (i.e. the catalyst saturation is reached) the NO inlet concentration is switched off (near 2400 s); after the switch a tail is observed in the NO and NO_2 concentration profile, due to the desorption of weakly adsorbed NO_x species. A further very small NO desorption is observed when

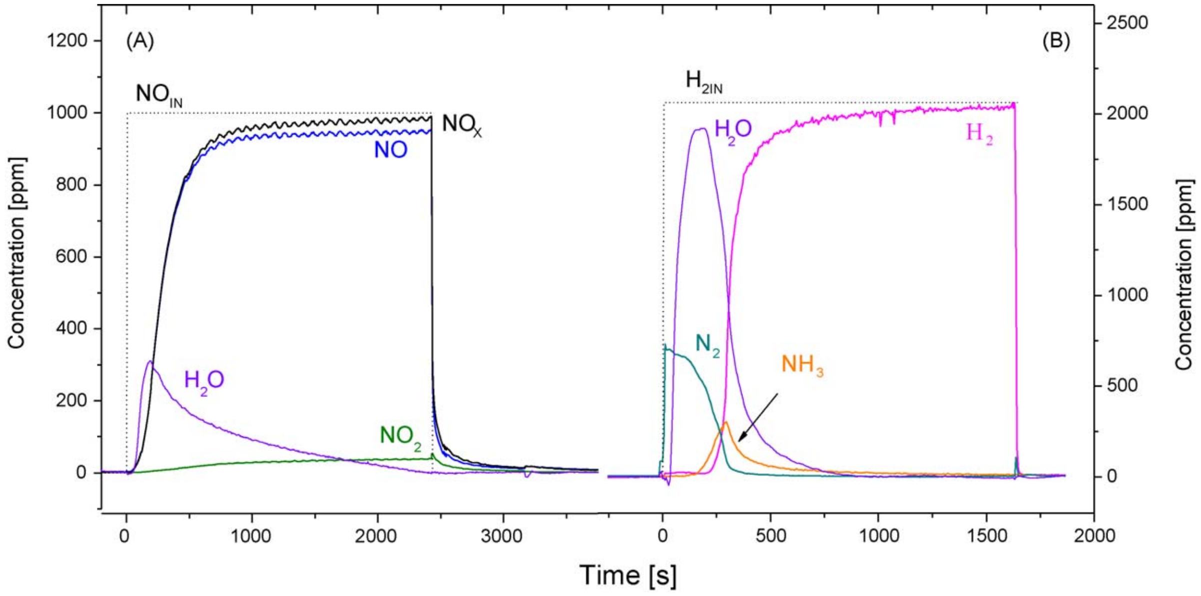

Fig. 1. (A and B) Lean-rich cycle carried out over Pt–Ba/Al_2O_3 catalyst sample at 200 °C. (A) Lean phase: 1000 ppm NO in He + 3% (v/v) O_2; rich phase: 2000 ppm H_2 in He. Catalyst loading 60 mg, flow rate 100 cm^3/min (at 1 atm and 0 °C).

the oxygen flow is stopped, in line with the O_2 partial pressure effect on the adsorbed species stability onto the catalyst surface [8].

The amount of stored NO_x at this temperature (200 °C) is near 3.45×10^{-4} mol/g_{cat}. This corresponds to an overall Ba utilization (i.e. the fraction of Ba involved in the storage to the overall Ba content of the catalyst, by assuming the formation of either $Ba(NO_2)_2$ or $Ba(NO_3)_2$) close to 12%, in line with previous results from our lab [17].

The results obtained upon reduction with H_2 at 200 °C of the NO_x stored at the same temperature are shown in Fig. 1B. H_2 is completely consumed upon its admission to the reactor; the H_2 breakthrough is observed near 210 s. N_2 formation is immediately observed upon H_2 admission, and after roughly 140 s large quantities of ammonia are also detected. Water is also formed during reduction, whereas no appreciable amounts of other products (e.g. NO and N_2O) are observed at the reactor outlet.

Accordingly at this temperature the average N_2 selectivity of the reduction, estimated according to Eq. (b), is near 81%. The N_2 selectivity increases when the experiments are carried out at higher temperatures (data not reported), in line with previous findings [10,13,14].

The overall H_2 consumption and the corresponding NH_3 and N_2 formation is due to the reduction of the adsorbed NO_x species, according to the stoichiometry of the following global reactions:

$$Ba(NO_2)_2 + 6H_2 \rightarrow 2NH_3 + BaO + 3H_2O \qquad (4)$$

$$Ba(NO_2)_2 + 3H_2 \rightarrow N_2 + BaO + 3H_2O \qquad (5)$$

$$Ba(NO_3)_2 + 8H_2 \rightarrow 2NH_3 + BaO + 5H_2O \qquad (6)$$

$$Ba(NO_3)_2 + 5H_2 \rightarrow N_2 + BaO + 5H_2O \qquad (7)$$

Reactions (4)–(5) and (6)–(7) account for the reduction of nitrites and nitrates, respectively, to NH_3 and N_2. Notably, in reactions (4)–(7) the formation of BaO is envisaged; as pointed out in [8], $Ba(OH)_2$ is also formed by reaction of BaO with H_2O according to the following reaction:

$$BaO + H_2O \rightarrow Ba(OH)_2 \qquad (8)$$

The formation of $Ba(OH)_2$ species during the reduction of stored NO_x is confirmed by the release of water upon NO addition to the catalyst in the adsorption (lean) phase, as previously discussed (Fig. 1A).

According to stoichiometries (4)–(7), different amounts of H_2 are consumed when N_2 and NH_3 formation is associated to the reduction of either nitrites (reactions (4) and (5)) or nitrates (reactions (6) and (7)). On the basis of the molar ratio between the amounts of evolved $N_2 + NH_3$ and of consumed H_2, from stoichiometries (4)–(7) the ratio nitrites/nitrates in the stored NO_x can be estimated, if one neglects any H_2 consumption via other routes (e.g. the reduction of PtO to Pt). Indeed, it is estimated that this contribution is at least one order of magnitude lower than that involved in the reduction of the stored NO_x. Calculation showed that at 200 °C the amount of nitrites accounts for the majority of the overall stored NO_x. This is in line with previous FTIR studies on the adsorption of NO_x over the same catalytic systems showing the presence of a large fraction of nitrites when the adsorption is carried out at low temperatures [25]. Accordingly it is concluded that at 200 °C reactions (4) and (5) account for the larger fraction of the overall H_2 consumption.

It is also worth to note that the N_2 concentration level near 690 ppm, observed at the beginning of the run, when H_2 is completely consumed, is consistent with the presence of nitrites. Indeed this concentration is very similar to that expected from the reduction of nitrites by 2000 ppm of H_2 (reaction (5), 667 ppm) and it is higher to that expected in the case of the reduction of nitrates (reaction (7), 400 ppm).

Notably, during the reduction of the stored NO_x, NH_3 is also formed (Fig. 1B). NH_3 evolution follows that of N_2, in line with several reports [11,12,26]. In previous papers from this group [10,13,14], it has been demonstrated that ammonia is an intermediate in the N_2 formation during the stored NO_x reduction with H_2. In particular, it has been shown that the reduction of nitrates stored onto the catalytic surface occurs according to a 2-step in-series mechanism [10,13,14]: in the first step, the reductant (i.e. H_2) reacts with nitrates to give NH_3 (reaction (6)); the so-formed ammonia reacts with the adsorbed NO_x to give N_2 (reaction (9)):

$$3Ba(NO_3)_2 + 8H_2 \rightarrow 2NH_3 + BaO + 5H_2O \quad (6)$$

$$3Ba(NO_3)_2 + 10NH_3 \rightarrow 8N_2 + 3BaO + 15H_2O \quad (9)$$

The sum of reactions (6) and (9) accounts for the overall stoichiometry of reduction of nitrates with hydrogen to give N_2 (reaction (7)). A similar pathway is suggested for the reduction of nitrites (overall reaction (5)). Notably, the temporal evolution of the reduction products, with nitrogen being detected at the reactor outlet first and ammonia later, is in line with the integral behaviour of the catalytic bed (plug-flow reactor), as demonstrated in [10,13,14]. As discussed also by Cumaranatunge [12] and Pihl [26], upon regeneration an hydrogen front travels along the catalyst bed. NH_3 is formed at the H_2 front upon reaction of H_2 with the stored NO_x; the formed NH_3 reacts with NO_x stored downstream the H_2 front, leading to the formation of N_2, which is immediately detected at the reactor outlet. When the front reaches the end of the catalytic bed, there are no NO_x stored downstream and this leads to the evolution of ammonia, which follows that of N_2. Besides, at the investigated temperature (200 °C), the reaction of ammonia with the stored NO_x is slow and this leads to the evolution of significant amounts of ammonia [11,12,26–28].

3.2.2. NO_x storage–reduction over FeZSM-5 catalyst

The catalytic behaviour of the FeZSM-5 SCR catalytic system has also been investigated under lean-rich conditions for comparison purposes. Accordingly ISC experiments have been performed following the same procedure already adopted for the Pt–Ba/Al_2O_3 catalyst.

Fig. 2 shows the results of a storage–reduction cycle carried out at 200 °C over the conditioned FeZSM-5 catalyst sample. Upon the NO step addition (Fig. 2A), the NO concentration immediately reaches the inlet value. NO_2 production is also observed, due to NO oxidation over Fe sites [29]. The NO flow is maintained for a while (2300 s) and then the inlet NO concentration is decreased to zero. The NO signal shows a small tail and then reaches the background level. The amounts of NO_x which have been stored are very low, near 5.3×10^{-5} mol/g_{cat}, in line with previous works [30]. In the subsequent reduction step with H_2 (Fig. 2B), the small amounts of adsorbed NO_x species are reduced to nitrogen and NO, which are detected at the reactor outlet; no ammonia has been observed.

3.2.3. SCR reactivity over FeZSM-5 catalyst

The FeZSM-5 SCR catalyst has also been tested at 200 °C in the SCR reaction under cyclic conditions, by admitting to the reactor pulses of NH_3 and of NO in the presence of O_2, with an inert purge in between.

Upon NH_3 admission to the reactor (1000 ppm in He, Fig. 3A), the NH_3 breakthrough is observed near 245 s. When a steady value of NH_3 concentration is reached (i.e. when the surface is saturated), the ammonia feed is closed. This leads to a significant desorption of ammonia. It is worth to note that the NH_3 desorption as a consequence of the pulse shutoff is quite relevant: as a matter of fact, only the 50–70% of the adsorbed ammonia remains on the catalytic surface in the absence of gaseous NH_3. The variation of the adsorbed NH_3 as a function of time during the whole test is shown in Fig. 4. Nevertheless the amounts of NH_3 adsorbed on the zeolite catalyst sample at the end of the adsorption procedure (4500 s) are significant, being near to 7.8×10^{-4} mol/g_{cat}.

Then a pulse of NO (1000 ppm) has been admitted to the reactor, in a flow of He + O_2 (3%, v/v), and results are shown in Fig. 3B.

As the oxygen has been admitted to the reactor inlet (t = 4600 s), a small N_2 peak is observed, due to the oxidation of stored ammonia. The observed N_2 amounts correspond to about 2% of the initially adsorbed NH_3. Then, when NO is added to the reactor, ammonia stored on the FeZSM-5 SCR catalyst is involved in the reduction of gaseous NO_x, as revealed by the relevant N_2 (and water) formation which accompanies the NO consumption (see Fig. 3B). The NO consumption and the N_2 formation are in line with the occurrence of the SCR reaction (1):

$$4NO + 4NH_3 + O_2 \rightarrow 4N_2 + 6H_2O$$

No other species have been detected during the reaction.

When the nitrogen concentration decreases and the NO signal increases, NO_2 is detected at the reactor outlet, with a time delay of about 700 s from NO admission. The presence of NO_2 is in line with

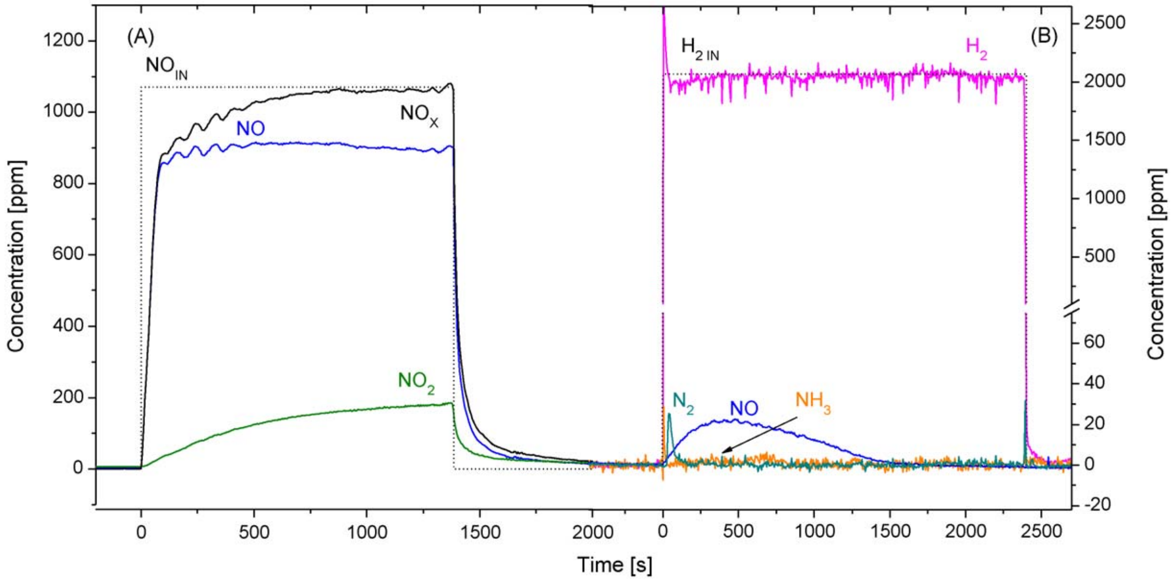

Fig. 2. (A and B) Lean-rich cycle carried out over FeZSM-5 catalyst sample at 200 °C. (A) Lean phase: 1000 ppm NO in He + 3% (v/v) O_2; (B) rich phase: 2000 ppm H_2 in He. Catalyst loading 60 mg, flow rate 100 cm^3/min (at 1 atm and 0 °C).

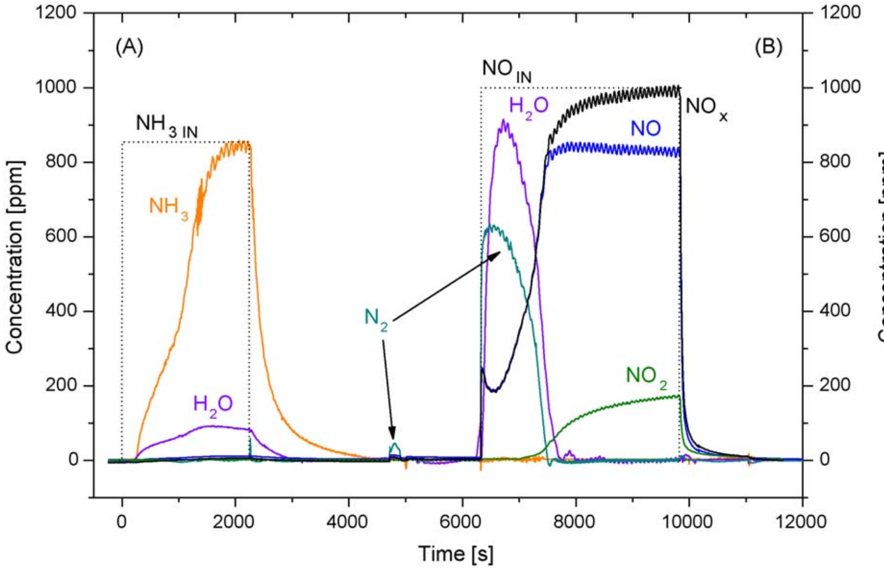

Fig. 3. (A and B) SCR reactivity test carried out over FeZSM-5 catalyst sample at 200 °C. (A) Rich phase: 1000 ppm NH_3 in He; (B) lean phase: 1000 ppm NO in He + 3% (v/v) O_2. Catalyst loading 60 mg, flow rate 100 cm^3/min (at 1 atm and 0 °C).

the oxidation capacity of the catalytic system as discussed during the LNT experiments (Fig. 2). Notably, in the absence of pre-adsorbed NH_3, NO_2 evolution does not show any delay (see Fig. 2A). In this case, the presence of a delay in the detection of NO_2 could be related to the involvement of this specie in the reaction of NO with the stored NH_3, according to the fast-SCR reaction (2). Hence it is speculated that part of NO is oxidized to NO_2 also at the beginning of the NO pulse; however NO_2 is readily involved in the SCR reaction with the stored NH_3, in line with the greater reactivity of the fast-SCR reaction (2) at this temperature [31,32] if compared to the standard SCR pathway (1). Accordingly NO_2 is detected at the reactor outlet only when complete consumption of NH_3 has been reached.

The N_2 production is estimated to be near 7.4×10^{-4} mol/g_{cat}, in good agreement with the amounts of NH_3 stored at this temperature (7.4×10^{-4} mol/g_{cat}) and with the fact that a small fraction of NH_3 has been oxidized to N_2 upon oxygen admission at the beginning of the lean phase (t = 4600 s).

It is worth to note that upon NO admission to the reactor the nitrogen production passes trough a maximum that corresponds to a maximum in the NO consumption. As already pointed out in previous work by some of us [33] and in more recent papers [34,35] this behaviour could be ascribed to an inhibitory effect of NH_3 on the SCR reaction, especially at low temperature. Therefore, the presence of a high coverage of the zeolite surface under these conditions (at T = 200 °C, the stored amount of NH_3 is high) inhibits the reaction. As the NH_3 surface concentration decreases, the rate of the SCR reaction initially increases and eventually becomes zero when the NH_3 surface concentration is nill. The reaction is very selective to N_2, in line with literature indications.

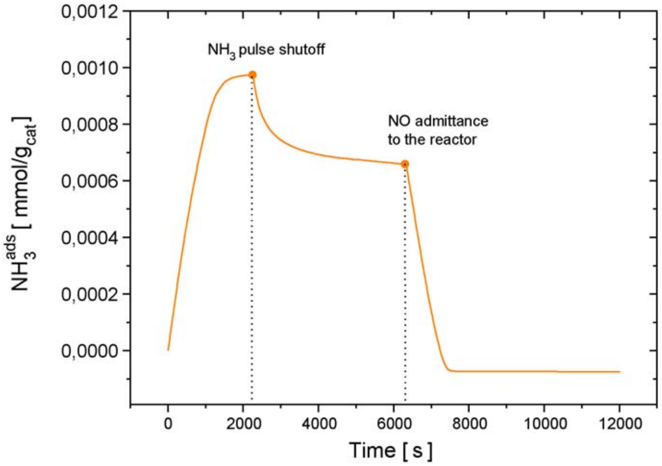

Fig. 4. Evolution of the amount of adsorbed ammonia on the zeolite sample as a function of time at 200 °C.

3.2.4. Lean-rich operations over a double-bed LNT + SCR reactor

NH_3 which is released from the LNT catalyst during rich operation (see Fig. 1B) can be stored on a SCR catalyst located downstream the LNT catalyst bed. As shown in Fig. 3, the stored ammonia can react with NO_x to produce N_2. To analyze these aspects, an in-series double-bed arrangement has been tested, in which a SCR sample (FeZSM-5) has been placed downstream the Pt–Ba/Al_2O_3 LNT catalyst. This catalyst configuration has been tested under the same experimental conditions adopted for the single Pt–Ba/Al_2O_3 LNT catalyst layer. Accordingly, ISC experiments were performed by alternating a feed of 1000 ppm of NO in the presence of O_2 (3%, v/v) and of 2000 ppm of H_2 in He with a He purge in between.

Fig. 5A and B show the results obtained during the NO_x storage–reduction experiments carried out over double-bed configuration at 200 °C. The data shown in Fig. 5 have been obtained after catalyst conditioning, until a reproducible behaviour is obtained in the lean-rich cycles.

Upon NO admission to the reactor (t = 0, Fig. 5A), the NO breakthrough is observed after 130 s. This is a higher value if compared to that observed in the case of the single-bed Pt–Ba/Al_2O_3 configuration (33 s, Fig. 1A). Then the NO_x concentration increases with time, but slowly if compared to the Pt–Ba/Al_2O_3 catalyst (compare Figs. 1A and 5A), so that at the end of the lean phase a higher amount of NO_x has been removed from the gas phase. Indeed the amounts of removed NO_x are near 6.13×10^{-4} mol/g_{cat}, vs. 3.85×10^{-4} mol/g_{cat} in the case of the single-bed configuration.

Notably, N_2 evolution is also observed during the lean phase, as opposite to what observed in the case of the single Pt–Ba/Al_2O_3 catalyst bed. N_2 formation is related in this case to the reaction between NH_3 (stored on the SCR catalyst bed during the previous

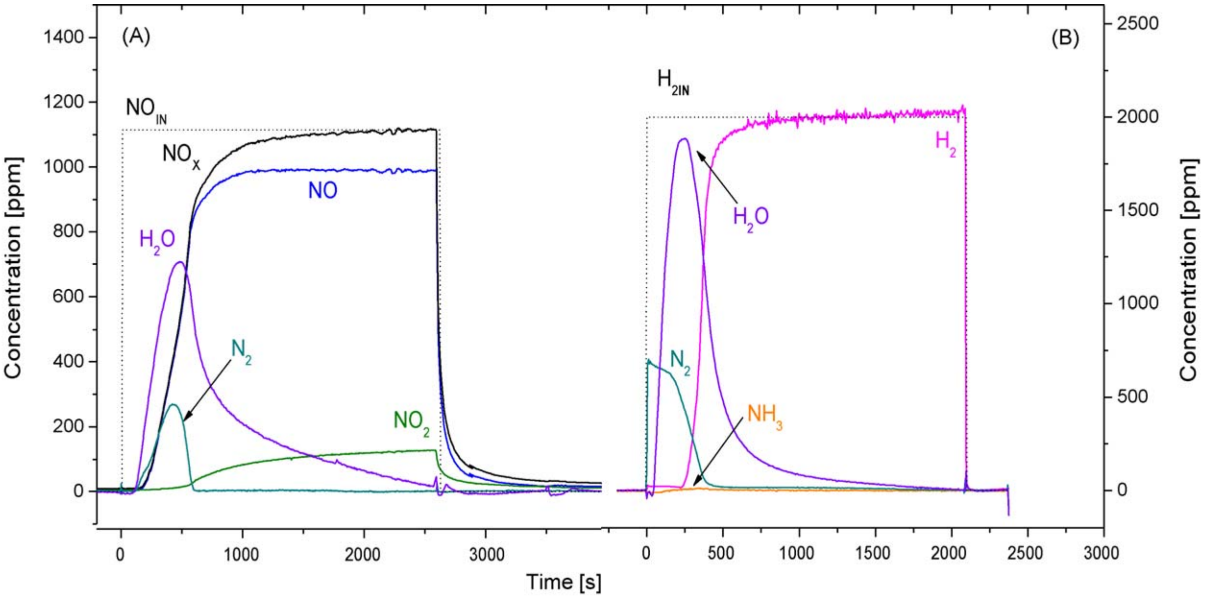

Fig. 5. (A and B) Lean-rich cycle carried out over a double-bed configuration (Pt–Ba/Al_2O_3–FeZSM-5 catalyst sample) at 200 °C. (A) Lean phase: 1000 ppm NO in He + 3% (v/v) O_2; (B) rich phase: 2000 ppm H_2 in He. Catalyst loading 60 mg + 60 mg, flow rate 100 cm^3/min (at 1 atm and 0 °C).

rich phase) and NO_x which escape from the Pt–Ba/Al_2O_3 catalyst bed placed upstream, according to the reactions (1) and (2):

$$4NO + 4NH_3 + O_2 \rightarrow 4N_2 + 6H_2O \quad (1)$$

$$NO + NO_2 + 2NH_3 \rightarrow 2N_2 + 3H_2O \quad (2)$$

Indeed, the amounts of N_2 produced during the lean phase (9.45×10^{-5} mol/g_{cat}) are in line with the amount of ammonia produced by LNT system in the case of the single-bed configuration (9.06×10^{-4} mol/g_{cat}, Fig. 1B). The occurrence of the SCR reaction is also pointed out by the detection of significant amounts of water during the lean phase.

Accordingly the amounts of NO_x removed from the gas phase are those adsorbed over the LNT sample, and those that reacted with ammonia adsorbed on the zeolite catalyst layer to give N_2 according to the SCR reaction. The stored NO_x have been calculated as the difference between the removed NO_x and the NO_x converted to N_2 (Eq. (a)), according to the SCR stoichiometry (reaction (1)). At 200 °C, these amounts are equal to 5.2×10^{-4} mol/g_{cat} in the case of the double-bed, and are consistent with the removed NO_x in the case of the single-bed configuration (i.e. 3.8×10^{-4} mol/g_{cat}).

Finally, NO_2 formation due to the oxidation of NO in the presence of oxygen and catalyzed by Pt and FeZSM-5 also takes place. Notably, NO_2 evolution is seen only after N_2 formation, with a time delay of about 440 s. As previously discussed, this is likely due to the involvement of NO_2 in the fast-SCR reaction. Indeed NO_2 which is formed over the NSR catalyst layer reaches the SCR catalysts and reacts with adsorbed NH_3, along with NO, according to the stoichiometry of the fast-SCR reaction (2). Since this reaction is faster than the standard SCR reaction (1) [18,19], NO_2 breakthrough is observed after that of NO, i.e. when the consumption of adsorbed ammonia is complete.

Finally, it is worth noticing that N_2 appears with a time delay near to 120 s with the respect to the NO admission. This feature is related to the sequence through which the two catalytic beds are arranged, i.e. with the Pt–Ba/Al_2O_3 system placed upstream the FeZSM-5 catalyst. In fact, NO_x reach the FeZSM-5 catalyst layer only after the NO_x breakthrough on the NSR catalyst bed, giving N_2 by reaction with the stored ammonia. Accordingly, nitrogen production is delayed if compared to NO admission to the reactor.

After adsorption at 200 °C, the stored NO_x have been reduced with H_2 at the same temperature (Fig. 5B). As shown in the figure, initially H_2 is completely consumed and the breakthrough is observed after 230 s. Upon H_2 admission the evolution of N_2 is immediately observed at the reactor outlet, along with negligible amounts of NH_3. Accordingly the selectivity to N_2 of the reduction phase is almost complete. Water is also formed during reduction, whereas no appreciable amounts of other products (e.g. NO and N_2O) have been observed. Note that these results are almost superimposed to those observed in the case of the single Pt–Ba/Al_2O_3 catalyst layer (compare Figs. 1B and 5B), but the amounts of ammonia observed in the double-bed configuration are negligible (0.12×10^{-5} mol/g_{cat} vs. 8.9×10^{-5} mol/g_{cat}), clearly indicating that NH_3 evolved from the Pt–Ba/Al_2O_3 catalyst is stored on the FeZSM-5 SCR catalyst layer placed downstream. Accordingly, in the case of the double-bed configuration, the measured H_2 consumption is higher than the theoretical one calculated from the stoichiometry of reactions (4)–(7), i.e. from the actual NH_3 and N_2 evolution at the reactor outlet. In fact hydrogen is consumed to give ammonia and N_2 from nitrites/nitrates, but NH_3 is not observed at the reactor outlet because it is stored onto the SCR catalyst.

Similar results have been obtained by Corbos et al. [18] who analyzed a double-bed catalytic system, with Pt–RhBa/Al_2O_3 upstream and CuZSM-5 downstream. They showed that the NO_x removal activity using two catalytic beds is higher than that of the single Pt–RhBa/Al_2O_3 catalyst. They ascribed the results to the occurrence of the NH_3-SCR reaction on the CuZSM-5 catalyst located downstream of the Pt–RhBa, in agreement also with previous results [15].

3.2.5. Lean-rich operations over a LNT + SCR physical mixture reactor

Finally, the reactivity of a catalyst sample made up by a physical mixture of equal amounts of Pt–Ba/Al_2O_3 and FeZSM-5 catalyst has been considered. The results obtained in a sequence of lean-rich cycles are displayed in Fig. 6.

As apparent from Fig. 6A, upon NO admission NO_x are immediately observed at the reactor outlet without any time delay. However the NO concentration slowly increases with time reaching a steady state value at 1500 s. NO_2 evolution is also

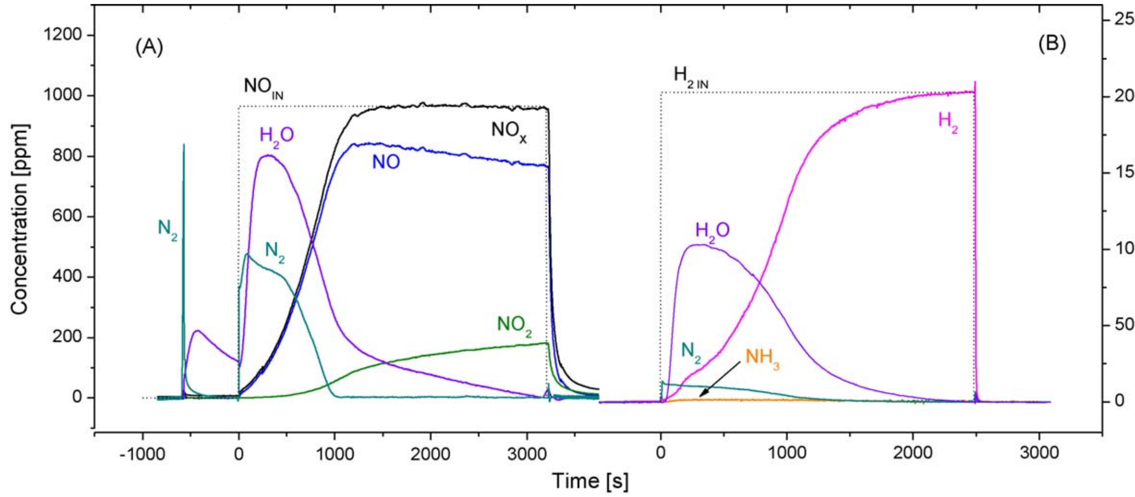

Fig. 6. (A and B) Lean-rich cycles carried out over a physical mixture configuration ($Pt–Ba/Al_2O_3$–FeZSM-5 catalyst sample) at 200 °C. (A) Lean phase: 1000 ppm NO in He + 3% (v/v) O_2; (B) rich phase: 2000 ppm H_2 in He. Catalyst loading 60 mg + 60 mg, flow rate 100 cm^3/min (at 1 atm and 0 °C).

observed, with a time delay near 510 s; the production of NO_2 is due to the occurrence of the NO oxidation reaction (3).

Notably, during the NO_x storage phase, a relevant N_2 production is also observed. N_2 evolution is immediately observed upon NO admission to the reactor, as opposite to what observed in the double-bed configuration (Fig. 5A) where N_2 evolution was delayed with respect to NO admission. Also in this case N_2 formation is due to the reaction of NO_x with ammonia which has been stored on the SCR catalyst particles during the previous rich phase. Since in this reactor configuration the FeZSM-5 sample is evenly distributed in the catalyst bed, upon NO admission to the reactor the NO adsorption/oxidation on the NSR catalyst to give NO_x adsorbed species (nitrites/nitrates), and the reaction of NO (and NO_2) with NH_3 adsorbed on the SCR catalyst to form N_2 occur simultaneously.

After the NO shutoff, a tail is observed in the NO_x trace due to the desorption of the weakly adsorbed NO_x species, as already discussed in the case of single-bed $Pt–Ba/Al_2O_3$ catalyst (Fig. 1A).

Note that in Fig. 6A, before the NO admission, a peak of N_2 (and of negligible amount of N_2O, not reported in the figure) is observed in the correspondence of the oxygen admission to the reactor ($t = -500$ s). This is likely due to the oxidation of ammonia stored on the SCR catalyst particles, in line with the behaviour of FeZSM-5 system during the SCR reactivity tests. Besides, in this case the amount of N_2 is higher than in the case of the double-bed due to the higher amount of ammonia stored onto the physical mixture.

Fig. 6B shows the subsequent reduction phase with H_2 (2000 ppm) in He at 200 °C. H_2 is completely consumed upon its admission to the reactor; but after only 36 s the H_2 breakthrough is observed. Then the H_2 concentration slowly increases with time, reaching the inlet value after 2000 s. N_2 evolution is observed upon H_2 admission, along with small but not negligible amount of ammonia (2.46×10^{-5} mol/g_{cat}). As already discussed for the double-bed configuration (Fig. 5B), the overall H_2 consumption measured in this case is much higher than the theoretical one calculated according to the stoichiometry of reactions (4)–(7) from the actual NH_3 and N_2 evolution at the reactor outlet, due to the trapping of ammonia on the SCR catalyst.

A comparison with the results of the double-bed arrangement (Fig. 5B) points out that in the case of the physical mixture the N_2 formation in the rich phase is much lower (1.25×10^{-4} mol/g_{cat} vs. 2.49×10^{-4} mol/g_{cat}). This could be explained on the basis of the suggested mechanism for N_2 production, in which ammonia is intermediate in the formation of N_2 [10]. As discussed above, over the LNT catalyst NH_3 is formed upon reaction of the adsorbed NO_x with H_2 and reacts with NO_x stored downstream the H_2 front leading to N_2. In the physical mixture system, the FeZSM-5 catalyst particles are homogeneously distributed in the catalyst bed and trap ammonia which is formed on the NSR catalyst particles during the rich phase. This prevents ammonia to react with NO_x stored downstream to give N_2 during the rich phase. Worth to note that being ammonia intermediate in the N_2 formation, the NH_3 trapping carried out by the FeZSM-5 catalyst during the catalyst regeneration blocks the formation of N_2 but not the reduction of the stored NO_x to NH_3. Accordingly the actual H_2 consumption is much higher than that expected from the observed N_2 and NH_3 formation according to reactions (4)–(7), since relevant amounts of NH_3 are stored on the SCR catalyst. This is indeed pointed out by the large N_2 formation which is observed during the lean phase (see Fig. 6A).

Finally Fig. 7 compares the amounts of NO_x removed in a lean/rich cycle for the investigated catalyst configurations, along with the amounts of NO_x stored, N_2 produced in the different phases, ammonia slip and N_2 selectivity. As previously reported, the amounts of the stored NO_x have been estimated by Eq. (a) by subtracting to the amounts of the overall consumed NO_x the amounts of NO_x consumed via the SCR reaction (estimated from the N_2 production during the lean phase).

Whereas the amounts of NO_x stored on the various catalyst configurations are roughly comparable, ranging from 3.9×10^{-4} to

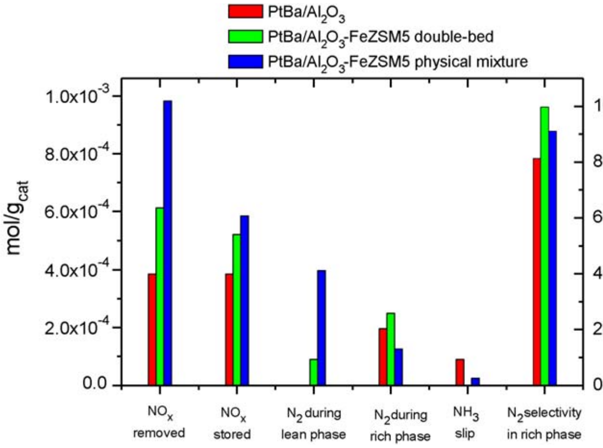

Fig. 7. NO_x removed, NO_x stored, N_2 during lean and rich phase, NH_3 slip, N_2 selectivity in the rich phase for the three reactor configurations (single-bed, double-bed and physical mixture).

5.8×10^{-4} mol/g_{cat}, worth to be noted is that the three investigated catalytic configurations show very different NO_x removal activity values. Accordingly, as apparent in Fig. 7, the NO_x removal activity of the Pt–Ba/Al_2O_3 + FeZSM-5 physical mixture is roughly three times that of the single Pt–Ba/Al_2O_3 catalyst, and it is also higher than that of the double-bed in-series configuration. Similar conclusions have been reported by Corbos et al. [18,19], who in fact showed that when H_2 is used as reductant the NO_x removal activity of a Pt–RhBa/Al_2O_3 LNT catalyst is greatly enhanced by coupling with a CuZSM-5 sample, both when the zeolite sample is placed downstream the Pt–RhBa/Al_2O_3 (double-bed) and when it is physically mixed. The increase in the NO_x efficiency has been ascribed by the Authors to the NO consumption with NH_3 formed on the Pt–RhBa/Al_2O_3 catalyst and trapped on the zeolite SCR catalyst. As a matter of fact our results show that ammonia formed during the rich phase and trapped over the zeolite SCR catalyst (no matter if the SCR catalyst is placed downstream or mixed with the NSR catalyst) can be efficiently exploited in the reduction of NO_x during the subsequent lean phase, with formation of N_2. However, since higher amounts of ammonia can be trapped in the case of the Pt–Ba/Al_2O_3–FeZSM-5 physical mixture rather than the double-bed configuration, a higher NO_x removal efficiency is measured in this case (see Fig. 7). At variance with our results, Corbos et al. [18,19] concluded that the physical mixture and the double-bed configuration lead to similar catalytic performances. The apparent discrepancies between our results and those of Corbos et al. [18,19] might be related, e.g. to the different experimental conditions used in this study, i.e. diluted isothermal conditions vs. lean-rich cycles with high reductant concentration (2000 ppm vs. 64,000 ppm H_2).

Fig. 7 also compares the N_2 production occurring during both the lean and the rich phases. The N_2 production during the rich phase is observed in all the three configurations, as expected, and is due to the reduction of NO_x stored onto the Pt–Ba surface. However, whereas the amounts of N_2 detected in the single and double-bed arrangement roughly correspond to the half of the stored NO_x, as expected according to the stoichiometry of reactions (5) and (7), in the case of the physical mixture the amounts of N_2 are significantly lower (1/3 of that expected). As discussed above, this is related to the fact that N_2 formation is prevented by the trapping onto the FeZSM-5 catalyst surface of ammonia which is formed upon reduction of the stored NO_x by H_2, and which is intermediate in N_2 formation. Accordingly, even though the NO_x stored onto the physical mixture are higher than in the other cases, the N_2 evolution during the rich phase is lower.

Finally, the N_2 production during the lean phase is observed only in the case of the double-bed and physical mixture, as consequence of the ammonia trapping on the FeZSM-5 catalyst. The nitrogen production is highest on the physical mixture due to the large amount of ammonia adsorbed in this case onto the zeolite surface, for the reasons already discussed. Notably, the trapping (during the rich phase) and the reaction (during the lean phase) of ammonia over the zeolite SCR catalyst also explain the low ammonia slip and the higher N_2 selectivity values which are observed in the case of the combined configurations (either double-bed or physical mixture), as shown in Fig. 7.

4. Conclusions

In the present work the behaviour in the reduction of NO_x under lean conditions of single Pt–Ba/Al_2O_3 LNT and FeZSM-5 SCR systems and of combined LNT + SCR configurations has been analyzed and compared under controlled isothermal conditions while analyzing the whole spectrum of reaction products. This allowed the decoupling of the various effects involved in the lean/rich cycles and a deeper understanding and rationalization of the chemical pathways occurring during the NO_x storage/reduction in the considered catalyst configurations.

It has been found that the presence of a SCR catalyst placed downstream the NSR catalyst bed (double-bed configuration) allows the storage of ammonia released during the rich phase on the LNT sample. The adsorbed ammonia is then converted to N_2 in the subsequent lean phase, according to the occurrence of a SCR reaction involving the stored ammonia and NO/NO_2 released from the front LNT catalyst layer. This increases both the NO_x removal efficiency and the N_2 selectivity of the process as well.

When the zeolite SCR catalyst is mixed with the LNT sample (physical mixture), a significant improvement of the NO_x removal efficiency is observed. This is due to the fact that during the rich phase, NH_3 which is formed on the LNT catalyst particles upon reaction of the adsorbed NO_x with H_2, is trapped on the SCR catalyst particles which are homogeneously distributed in the catalytic LNT/SCR layer. In line with the role of ammonia as intermediate in N_2 formation, this NH_3 trapping mechanism prevents N_2 formation during the rich phase. Accordingly during the following lean phase, NO_x are stored on the LNT catalyst but they also react with ammonia stored on the SCR catalyst leading to significant N_2 evolution and to the observed significant increase of the NO_x removal efficiency. Hence in the combined catalyst configurations, both double-bed and mechanical mixture, the capacity of the SCR catalyst to adsorb ammonia formed over the LNT catalyst particles leads to the double benefit of reducing the ammonia slip and to increase the N_2 selectivity and the NO_x removal efficiency.

References

[1] T. Johnson, Platinum Met. Rev. 52 (2008) 23.
[2] A. Güthenke, D. Chatterjee, M. Weibel, B. Krutzsch, P. Kočí, M. Marek, I. Nova, E. Tronconi, Adv. Chem. Eng. 33 (2008) 103.
[3] R.Q. Long, R.T. Yang, J. Am. Chem. Soc. 121 (1999) 5595.
[4] A.Z. Ma, W. Grunert, Chem. Commun. 1 (1999) 71.
[5] W.S. Epling, L.E. Campbell, A. Yezerets, N.W. Currier, J.E. Parks, Catal. Rev. Sci. Eng. 46 (2004) 163.
[6] S. Matsumoto, Catal. Today 90 (2004) 183.
[7] I. Nova, L. Castoldi, L. Lietti, E. Tronconi, P. Forzatti, F. Prinetto, G. Ghiotti, J. Catal. 222 (2004) 377.
[8] L. Lietti, P. Forzatti, I. Nova, E. Tronconi, J. Catal. 204 (2001) 175.
[9] F. Prinetto, G. Ghiotti, I. Nova, L. Lietti, E. Tronconi, P. Forzatti, J. Phys. Chem. B 105 (2001) 12732.
[10] L. Lietti, I. Nova, P. Forzatti, J. Catal. 257 (2008) 270.
[11] S.S. Mulla, S.S. Chaugule, A. Yezerets, N.W. Currier, W.N. Delgass, F.H. Ribeiro, Catal. Today 136 (2008) 136.
[12] L. Cumaranatunge, S.S. Mulla, A. Yezerets, N.W. Currier, W.N. Delgass, F.H. Ribeiro, J. Catal. 246 (2007) 29.
[13] P. Forzatti, L. Lietti, I. Nova, Energy Environ. Sci. 1 (2008) 236.
[14] I. Nova, L. Lietti, P. Forzatti, Catal. Today 136 (2008) 128.
[15] H. Shinjoh, N. Takahashi, K. Yokota, Top. Catal. 42–43 (2007) 215.
[16] T. Nakatsuji, M. Matsubara, J. Rouistenmaki, N. Sato, H. Ohno, Appl. Catal. B 77 (2007) 190.
[17] P. Forzatti, L. Lietti, The reduction of NO_x stored on LNT and combined LNT–SCR systems, Catal. Today (2009), doi:10.1016/j.cattod.2008.11.023.
[18] E.C. Corbos, M. Haneda, X. Courtois, P. Marecot, D. Duprez, H. Hamada, Catal. Commun. 10 (2008) 137.
[19] E.C. Corbos, M. Haneda, X. Courtois, P. Marecot, D. Duprez, H. Hamada, Appl. Catal. A 365 (2009) 187.
[20] F. Frola, F. Prinetto, G. Ghiotti, L. Castoldi, I. Nova, L. Lietti, P. Forzatti, Catal. Today 126 (2007) 81.
[21] N. Miyoshi, T. Tanizawa, K. Kasahara, S. Tateishi, European Patent Application 0 669 157 A1, 1995.
[22] I. Nova, L. Castoldi, F. Prinetto, V. Dal Santo, L. Lietti, E. Tronconi, P. Forzatti, G. Ghiotti, R. Psaro, S. Recchia, Top. Catal. 30–31 (2004) 181.
[23] F. Frola, M. Manzoli, F. Prinetto, G. Ghiotti, L. Castoldi, L. Lietti, J. Phys. Chem. C 112 (2008) 12869.
[24] M.M.J. Treacy, J.B. Higgins (Eds.), Collection of Simulated XRD Powder Patterns for Zeolites, fourth revised edition, Elsevier, 2001.
[25] F. Prinetto, G. Ghiotti, I. Nova, L. Castoldi, L. Lietti, E. Tronconi, P. Forzatti, Phys. Chem. Chem. Phys. 5 (2003) 4428.
[26] A. Pihl, J.E. Parks II, C.S. Daw, T.W. Root, SAE Technical Paper, 2006-01-3441.
[27] W. Partridge, J.S. Choi, Appl. Catal. B 91 (2009) 144.
[28] R.D. Clayton, M.P. Harold, V. Balakotaiah, Appl. Catal. B 84 (2008) 616.
[29] M. Rivallan, G. Ricchiardi, S. Bordiga, A. Zecchina, J. Catal. 264 (2009) 104.
[30] A. Grossale, I. Nova, E. Tronconi, Catal. Today 136 (2008) 18.

[31] A. Kato, S. Matsuda, T. Kamo, F. Nakajima, H. Kuroda, T. Narita, J. Phys. Chem. 85 (1981) 4099.
[32] C. Ciardelli, I. Nova, E. Tronconi, B. Bandl-Konrad, D. Chatterjee, M. Weibel, B. Krutzsch, Appl. Catal. B 70 (2007) 80.
[33] I. Nova, L. Lietti, E. Tronconi, P. Forzatti, Catal. Today 60 (2000) 73.
[34] A. Grossale, I. Nova, E. Tronconi, D. Chatterjee, M. Weibel, J. Catal. 256 (2008) 312.
[35] A. Grossale, I. Nova, E. Tronconi, J. Catal. 265 (2009) 141.